47TH TURBOMACHINERY & 34TH PUMP SYMPOSIA
HOUSTON, TEXAS | SEPTEMBER 17-20, 2018
GEORGE R. BROWN CONVENTION CENTER

# SURGE EXPLORATION TESTS AND SECOND QUADRANT CHARACTERISTIC DYNAMIC MODELING ON FULL-SCALE CENTRIFUGAL COMPRESSOR

**Fabio Baldanzini**
Lead Engineer
Centrifugal Compressors & Turbo Expanders - System Operability
Baker Hughes, a GE company
Florence, Italy

**Mirco Calosi**
Lead Engineer
Centrifugal Compressors & Turbo Expanders - System Operability
Baker Hughes, a GE company
Florence, Italy

**Marco Pelella**
Engineering Manager
Centrifugal Compressors & Turbo Expanders - System Operability
Baker Hughes, a GE company
Florence, Italy

*Fabio is Lead Engineer for System Operability of Centrifugal Compressor & Turbo Expander Applications at BHGE, in Florence, Italy. His responsibilities include compressor train operability analysis and simulations, focusing on Centrifugal Compressors interaction with drivers and Oil & Gas process plants during normal and transient operating scenarios.*
*Fabio joined GE in 2010 as Design Engineer in Gas Turbine Flange to Flange Organization. Then he worked as String Test Project Engineer and Auxiliary System Mechanical Engineer. In 2012 he moved in the present position. Fabio received a M.S. degree with honor in Mechanical Engineering from University of Florence, Italy in 2009.*

*Mirco Calosi is Lead Engineer for System Operability of Centrifugal Compressor & Turbo Expander Applications at Baker Hughes, in Florence, Italy. His responsibility is to smoothly integrate Centrifugal Compressors and relevant drivers within the Oil & Gas plant to make sure all transient conditions are fully covered by the entire plant design. Mr. Calosi graduated with honor in Chemical Engineering at University of Pisa, Italy in 2008. He joined GE in 2014.*

*Marco Pelella is Engineering Manager for NPI Systems Engineering & Operability of Centrifugal Compressor & Turbo Expander Applications at Baker Hughes, in Florence, Italy. His responsibilities include the new product system and architecture definition, the definition of process control philosophies, development of dynamic simulations and optimization for Centrifugal Compressors and Turbo Expanders applications. He joined GE in 1999 as Centrifugal Compressors Design Engineer and covered several positions as Centrifugal Compressor Design Manager working on integrally geared compressors, pipelines, LNG and Down Stream applications until the 2014 when he took the present role. Mr. Pelella graduated with honor in Mechanical Engineering at University of Naples, Italy in 1997, he has authored and coauthored 8 papers in compressor field and he presently holds 10+ patents.*

## ABSTRACT

Surge exploration tests on a full-scale centrifugal compressor have been performed allowing an evaluation of the transient behavior and the mechanical robustness of the compressor even during a critical event such as surge.
Compressor surge has been analyzed under different conditions, forcing the operating point to move beyond the performance envelope in full speed, at low and high pressure levels, and during emergency shut-downs. Thanks to the complex arrangement of the gas loops and several valves used to recycle the compressed gas, different levels of surge intensity were induced upon emergency shut-down.
The explorations of a fast event like surge called for special instrumentation, configured to acquire process data both in forward and reverse flow conditions in the most reliable way, with a high frequency sampling for an oil and gas environment.
The result of this work is a breakthrough for the tuning of a centrifugal compressor model to be used for dynamic simulations and

prediction of compressor dynamics during surge events (like surge cycle frequency and absorbed torque during Second Quadrant operation) in a more reliable and robust way.
Surge exploration tests results analysis, in terms of vibrations and thrust loads, together with development of a compressor enhanced dynamic model, allowed a change from a surge acceptance criterion - based on the time spent on the left of the Surge Limit Line during an Emergency Shutdown event - to a more physics based criterion - based on the acceptable number of surge cycles, thus increasing selection optimization of additional protections, such as hot/cold gas bypass valves.

## 1 INTRODUCTION

A test campaign has been carried out to test the behavior of a full-scale centrifugal compressor beyond the First Quadrant envelope, focusing on the behavior at surge. This activity allowed evaluating the mechanical robustness of the compressor upon a critical event such as deep surge conditions (Second Quadrant operation).

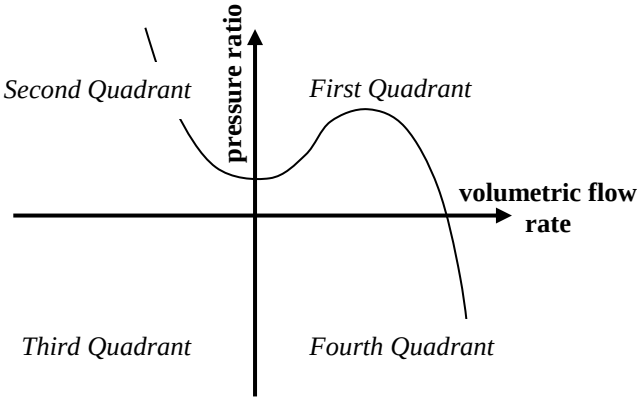


**Figure 1. Compressor Quadrants**

The tested compressor is a 3 section compressor, arranged in line with two, three and two impellers respectively. Figure 3 is a description of the test bed set for test campaign activity.

**Figure 2. Test bed arrangement at the BHGE Facility in Florence (Italy)**

The purpose of surge exploration tests was also to collect thermodynamic parameters beyond the First Quadrant compressor envelope. In particular, Second Quadrant operation and periodic surge cycles in which the compressor experiences a series of flow reversal and recovery, was deeply investigated in order to develop a reliable model - capable of predicting compressor behavior upon surge.

The paper is organized as follows: in section 2, the test bench gas loop and the instrumentation used are presented; section 3 describes the test campaign; in section 4 vibrations, axial displacements and thrust loads recorded during two runs of the test campaign are analyzed; section 5.1 describes the results of a model test performed on a single stage compressor, used to characterize the Second Quadrant map branch and how it has been adapted to the tested machine; in section 5.2 an overall gas loop dynamic simulation model is presented; section 5.3 deals with data validation between simulation results and test data; and finally, conclusions are given in section 6.

## 2 GAS LOOP ARRANGEMENT AND INSTRUMENTATION

The test loop arrangement consisted of three independent closed gas loops connected to each compressor section, equipped with recycle solenoid valves (ASVs) and a cooler at the suction. Bypass valves (PCV12 and PCV23, ball valve type) were installed to reproduce serial operation. Such a configuration (Figure 3) provided the maximum flexibility to test the full-scale compressor in several operational arrangements, also allowing for the decoupling of the three phases, as well as to study their mutual interactions during a surge event.
The compressor was coupled with a variable speed electric motor driver with 10 MW maximum available power.

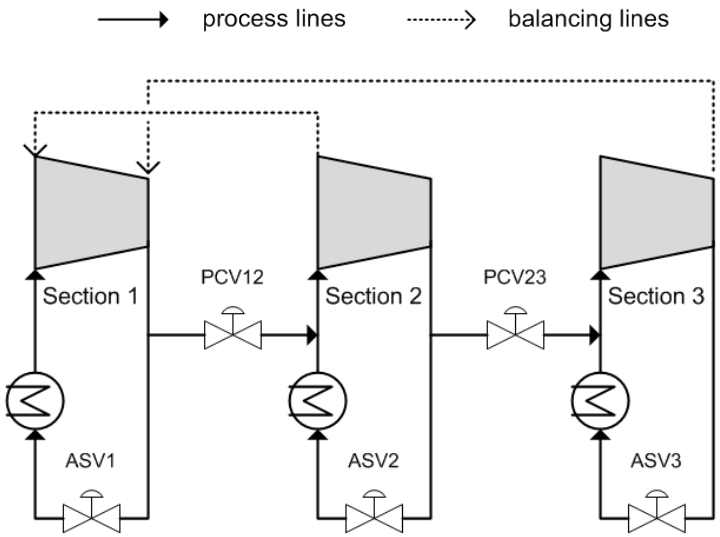


**Figure 3. Testing loop arrangement**

To evaluate surge both from the thermodynamic and mechanical standpoint, the test bed was equipped with dedicated instrumentation aimed at properly collecting data in forward and reverse flow operation conditions, also with suitable acquisition frequency for surge phenomena (10Hz for flows and pressures and 1Hz for temperatures). Four dynamic pressure transducers and four thermocouples were installed on the suction and discharge of each compressor section; flow rate measurement was performed by differential compressor section pressure transducers installed both on suction and discharge, with 2% of accuracy on design values. The ASME orifice plates on each discharge were installed reversed to acquire reverse flow across the compressor sections. Radial vibrations were measured through proximity probes located on both shaft ends with a 2000 Hz frequency response bandwidth. Axial displacements and axial thrust acting on the rotor were respectively measured through proximity probes and load cells installed on the thrust bearing.

## 3 SURGE EXPLORATION TESTS CAMPAIGN

Compressor surge has been analyzed under different operating conditions, forcing the operating point to move beyond the performance envelope at full speed and during emergency shut-downs, at low and medium gas loop pressures. The compressor control algorithm was modified to induce different levels of surge intensity upon Emergency Shut Down through an instantaneous (as per standard procedure), delayed and frozen recycle valve opening action.
Compressor surge at full speed was induced on a specific compressor section, by slowly closing the relevant ASV to increase the pressure ratio and reducing the flow until the operating point moved beyond the compressor envelope surge limit. In order to prevent any mutual effects upon surge, the two other compressor sections were kept operating far from surge limit, in the middle of the compressor envelope, close to the design point. In this way, surge cycles on each compressor section were evaluated.
Before and after each surge test, performance at a reference point condition was evaluated in order to capture any potential

degradation due to surge phenomena detrimental effects on the machine. Compressor performance at reference point was always met, again demonstrating that no detrimental effect due to surge on the compressor mechanical integrity was experienced.
The present work refers to a partially pressurized compressor loop, having compressor suction pressure at 5 barA and discharge at 60 barA. The following surge testes has been performed:

- ESD with all recycle valves kept at their initial opening position;
- Surge induced on section 1, closing the relevant ASV, at full speed;
- Surge induced on section 2, closing the relevant ASV, at full speed;
- Surge induced on section 3, closing the relevant ASV, at full speed.

A compressor mechanical analysis has been performed leveraging data relevant to the first two tests.
Data validation with the dynamic model results was completed on data relevant to all the four tests.

## 4 MECHANICAL TEST DATA ANALYSIS

Mechanical behavior has been analyzed in terms of radial vibrations, axial displacements and thrust load variations. Figure 4 reports compressor speed and radial vibrations evaluated through proximity probes located on NDE compressor side. The red line depicts the direct radial vibration, including all frequency spectrum contributions; the green one is the radial vibration at the rotational frequency (hereafter called in this study "1xRev"). Both trends have been normalized with respect to the value of the direct radial vibration at the initial steady state condition. In the initial steady state, these contributions were identical, an indication that radial vibrations were mainly due to rotor residual imbalance. Alternatively, during surge, non-synchronous vibrations were excited so that direct radial exceeded 1xRev vibrations. According to Figure 4, the former reached about 2.2 and the latter 1.8. Therefore, surge cycles were able to excite sub-synchronous vibrations for an amplitude close to 0.4. It should be noted that the maximum allowable threshold (1.7) was overcome without triggering trip. In order to disregard spurious data, a signal continuously above the threshold for at least 0.3 sec was required to initiate the ESD.
To detect the main contribution frequency to vibrations spectrum during surge, waterfall and spectrum plots were also developed for radial vibrations probes. As done with the other variables, vibration frequency has been normalized in the following figures with respect to the value at initial steady state conditions. Figure 5 highlights that rotor surge response was evident in the sub-synchronous range of 1xRev frequency and only during the flow reversal (from positive to negative) timeframe. A forced response on the first rotor mode is present within this range (at about 0.25) corresponding to the maximum spectrum contribution (red box in Figure 5).

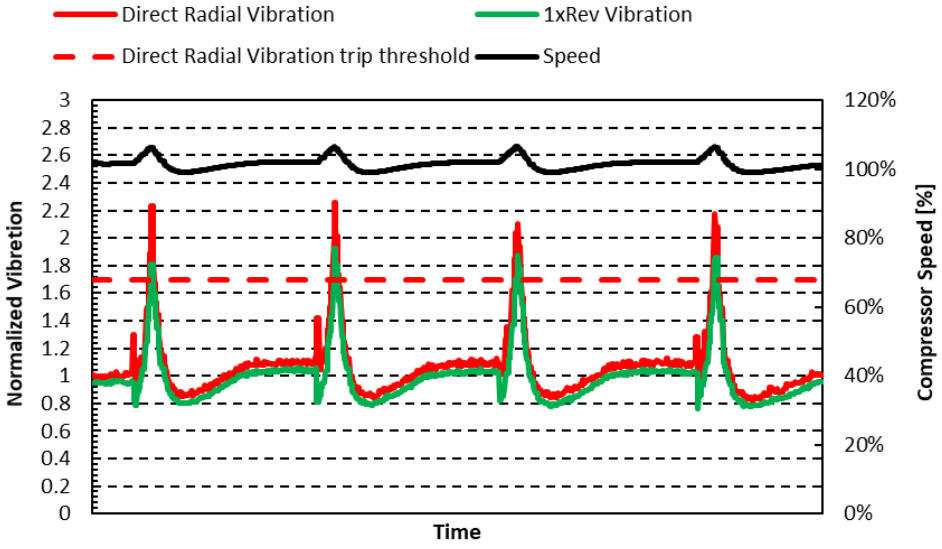


**Figure 4. First Section surge Cycles at full speed – Radial Direct and 1xRev vibration on NDE trends and compressor speed**

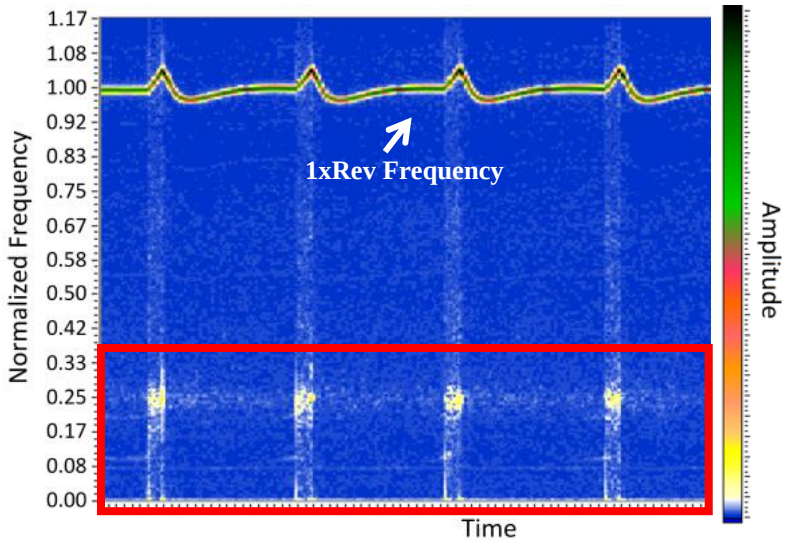


**Figure 5. First Section surge Cycles at full speed – Waterfall for Radial Direct Vibration on NDE**

The compressor speed variation was also deemed a key parameter for compressor behavior upon surge as it is an indication of the absorbed torque variation during the transient state. As the operating point moved in the Second Quadrant operation, the speed increased as an effect of a lower absorbed torque, reaching a maximum value while approaching the zero flow condition. Then, when the operating point moved back into First Quadrant, the absorbed torque started increasing, leading to a speed drop till its previous value was reached. It should be noted that speed variations were also affected by the speed controller, which was acting on electric motor torque trying to keep the speed at its set point. However, this effect is considered negligible on speed variation with respect to the compressor absorbed torque fluctuations due to surge.

The compressor surge behavior was also tested upon ESD, forcing all three sections to move in reverse flow conditions (Second Quadrant) by freezing the ASVs opening position so as to hinder the suction and discharge pressure equalization during coast down. Before initiating ESD, the three compressor sections were brought close to their Surge Limit Line (SLL) by closing ASVs. As soon as the ESD was triggered, speed started decreasing and reverse flows were detected in all three sections. As soon as the reverse flow condition across each compressor section occurred, direct radial vibrations showed a peak amplitude of 1.5 (126% of initial operation) as shown in Figure 6. The same increment was not present on the 1xRev component trend, an indication of a wider range of frequencies that was contributing to the overall vibration upon surge.

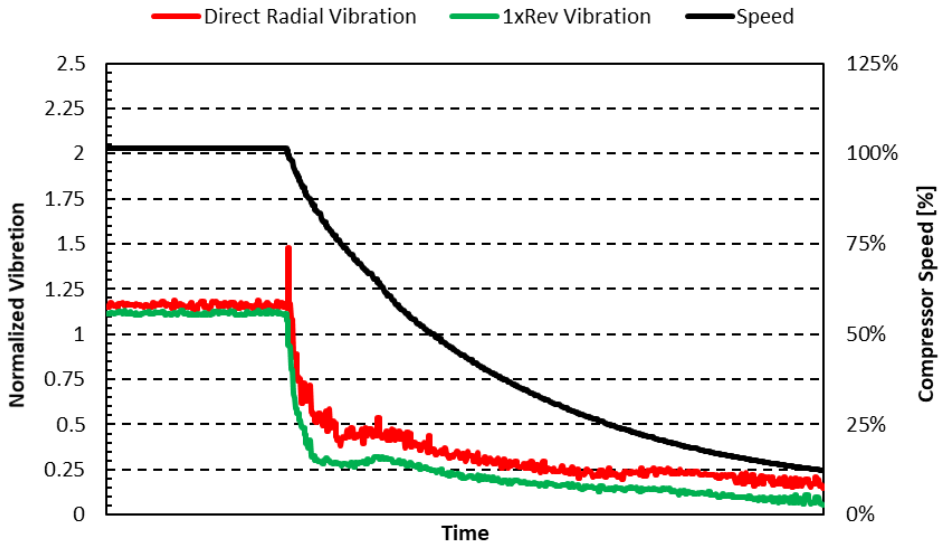


**Figure 6. Surge upon ESD – Radial Direct and 1xRev vibration trends on NDE and compressor speed**

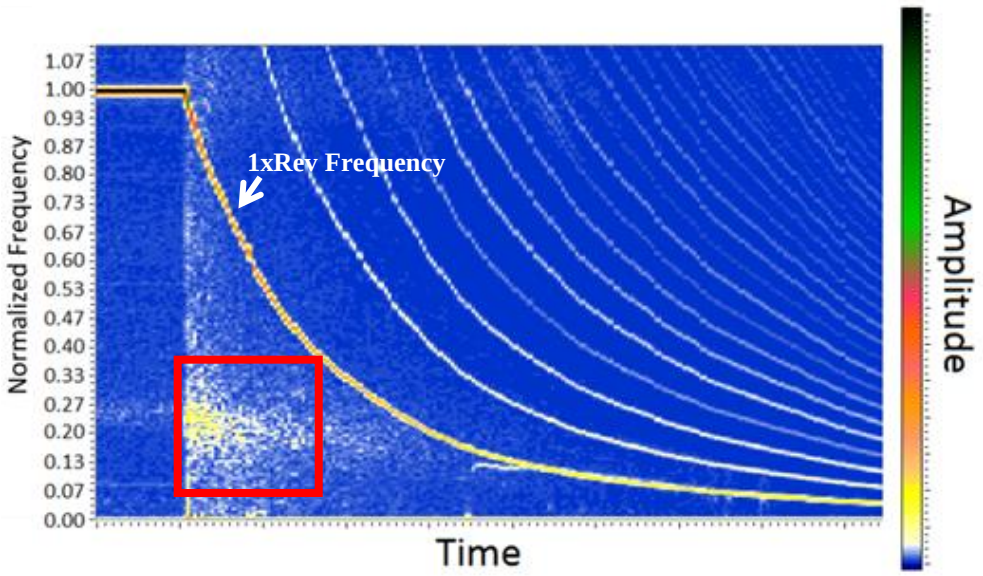


**Figure 7. Surge upon ESD – Waterfall for Radial Direct Vibration on NDE**

The waterfall plot in Figure 7 provides a further confirmation that surge is a "broadband" transient phenomenon. Vibration amplitudes decayed without any further peaks during the compressor coast down, an indication that reverse flow condition is an acceptable operation from a mechanical standpoint. With regards to the entire vibration spectrum, the same conclusions relevant to the surge tests at full speed can be drawn since sub-synchronous vibrations of a minor magnitude were observed (red box in Figure 7).
For the sake of completeness, axial displacements and axial thrust load were also evaluated, as done in [5]. Figure 8 and Figure 9 show these variables normalized with respect to the value at their own initial steady state condition. In case of surge under operating conditions, axial displacements and thrust load had a peak to 1.24 and 2.5 respectively (Figure 8), without exceeding the thrust bearing rated capacity.

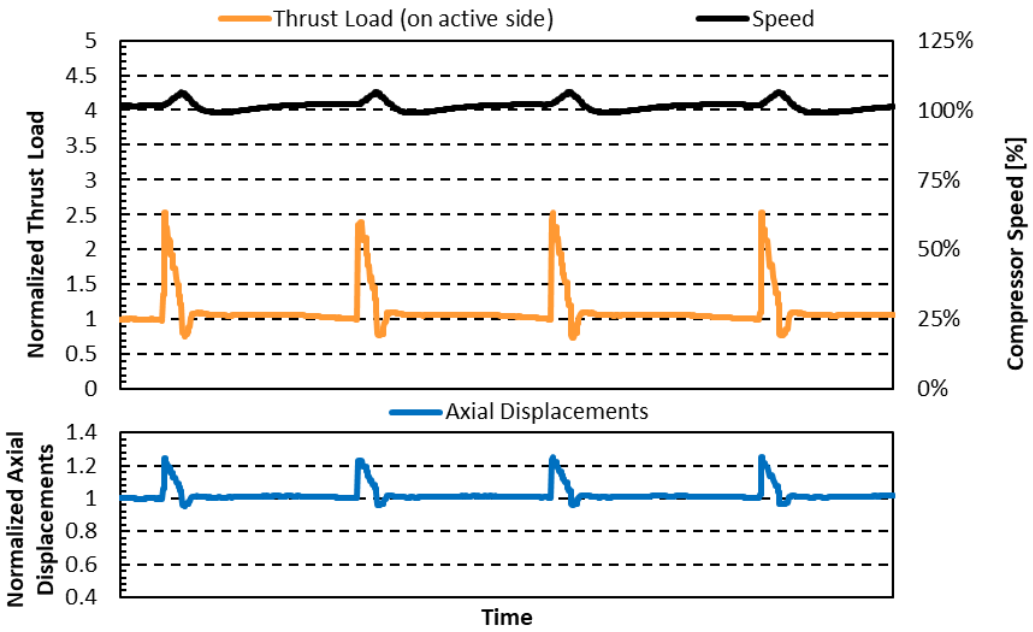


**Figure 8. Axial Displacements and Thrust Load on active side – surge Cycles at full speed**

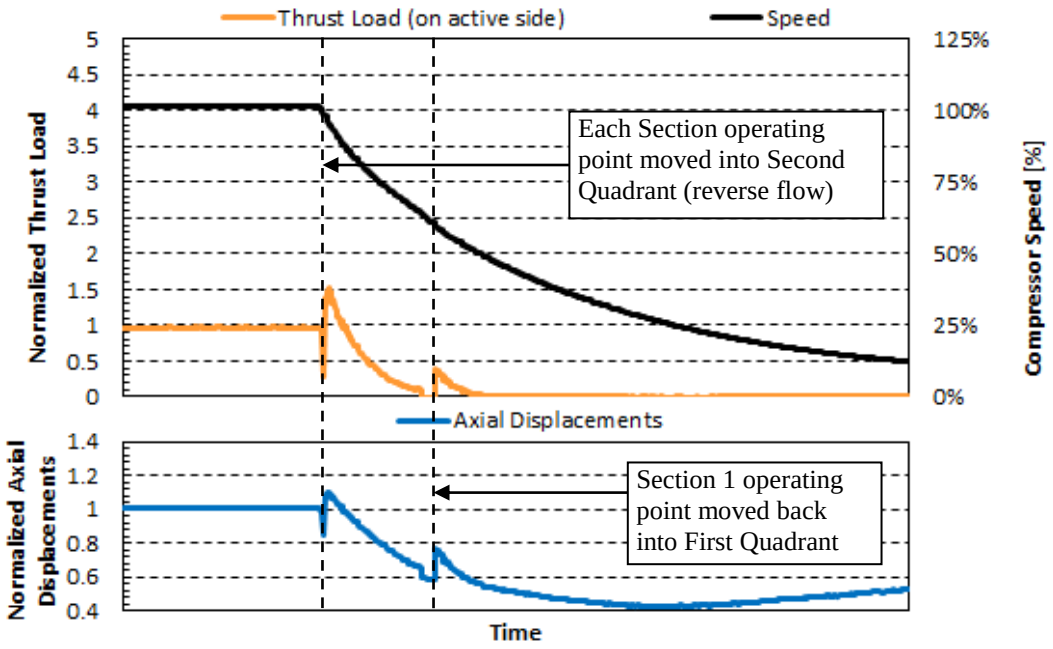


**Figure 9. Axial Displacements and Thrust Load on active side – surge upon ESD**

On surge during the ESD test, both axial displacements and thrust load decayed during the compressor coast down apart from two excursions experienced as soon as the operating point moved in the Second Quadrant region and when first section compressor returned from Second to First Quadrant operation (see Figure 9).
An important outcome of the surge exploration tests is that a reverse flow condition (aka Second Quadrant region) can be tolerated by the compressor, even for a prolonged period of operation (such as the entire compressor coastdown duration), since vibrations and axial thrust trends decayed smoothly. However, the surge phenomenon associated with reversing, oscillating flow, not only across the compressor but the entire compression system equipment (like scrubbers, coolers, valves, piping and relevant anchors, etc.), requires a threshold on the number of surge cycles to avoid undesirable upsets due to pressure waves and vibrations.
A new surge acceptance criteria has been developed accounting for a maximum of three surge cycles instead of operating time beyond the compressor Surge Limit Line (SLL) as per current commonly used design practice.
While the new approach to evaluate compressor surge is conservative, it is expected to reduce or prevent undue complexity such as installation of additional surge protection devices (like hot/cold gas bypass valve) or hardware modifications.

## 5 SURGE MODEL AND DATA MATCH

Another purpose of surge exploration testing was also to collect thermodynamic data relevant to the Second Quadrant operation to be compared with simulation results.
For this scope, compressor behavior has been simulated with a custom model based on a modified Moore-Greitzer [4] compressor dimensionless characteristic curve (cubic shape). The Second Quadrant map branch has been characterized with an ad-hoc Model Test carried out on a single stage compressor [2]. The model was then adapted on the tested full-scale compressor based on Surge Exploration Tests, the subject of this paper. Compressor map development in the Second Quadrant and surge tests data matching are described in the following sections.

### *5.1 Second Quadrant compressor model*

In the model test arrangement (which is more thoroughly investigated in [2] and [3]) a booster compressor was connected in series but opposed with the tested stage forcing the flow to be stable in reverse flow conditions (Figure 10).

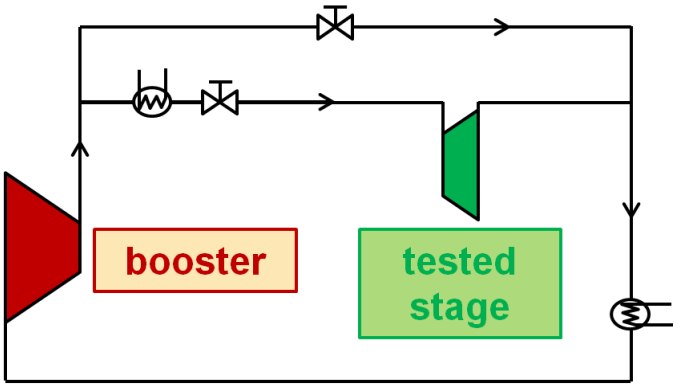


**Figure 10. Model Test Arrangement**

The trends of pressure ratio measured in the Second Quadrant are reported as a function of flow coefficient in Figure 11.

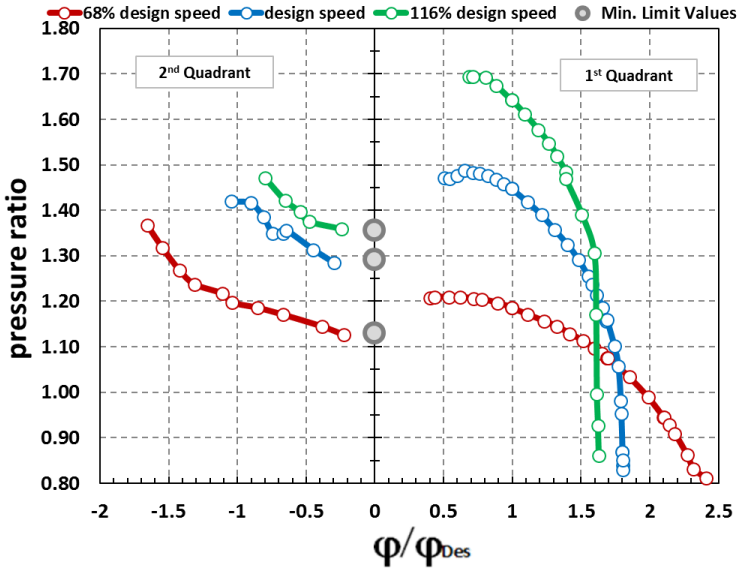


**Figure 11. Measured Performance in 1st and 2nd Quadrant**

$$\varphi = \frac{4\dot{m}}{\rho_{in}\pi D_2^2 u_2} \qquad \textbf{Eq. 1}$$

In the First Quadrant (positive flow), compressor curves display the commonly expected shape: with decreasing flow resulting in rising pressure ratio until it reaches the surge limit. In the Second Quadrant (negative flow), reducing the amount of reverse flow to zero, pressure ratio tends to a minimum limit value which corresponds to centrifugal forces at the imposed rotational speed. Compressor curve trends observed are in accordance with the cubic shaped compressor dimensionless characteristic curve of the Moore-Greitzer model (Figure 12) which has been taken, together with the equation of motion (Equation (2)) as reference for the development of the compressor dynamic model.

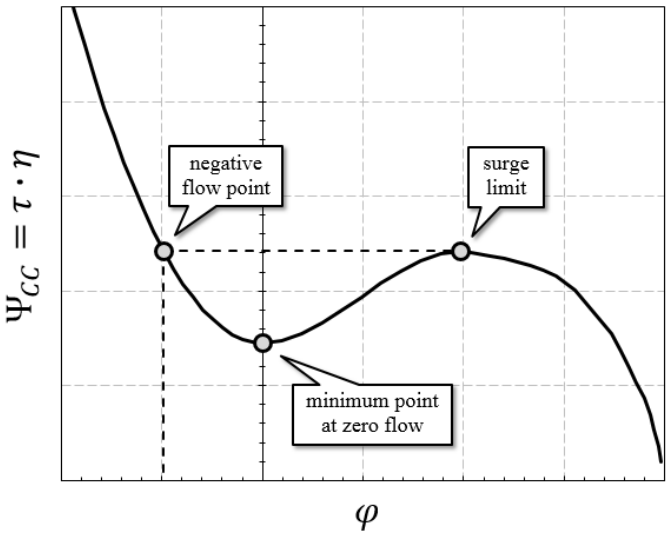


**Figure 12. Dimensionless Map in 1st and 2nd Quadrant**

$$\begin{cases} \eta_{pol} = f(\varphi) \\ \Psi_{CC} = \frac{H_{pol,CC}}{u_2^2} = f(\varphi) \\ \mathrm{H}_{pol,P} = f(T_{in}, P_{in}, P_{out}) \\ \frac{\partial \varphi}{\partial t} \propto \left(\mathrm{H}_{pol,CC} - H_{pol,P}\right) \end{cases} \qquad \textbf{Eq. 2}$$

In Equation (2), $H_{pol,P}$ is the polytropic head calculated from the process gas thermodynamic properties at the inlet and outlet section of the compressor, $\mathrm{H}_{pol,CC}$ is the polytropic head of the compressor given by the compressor map and $\eta_{pol}$ is the compressor polytropic efficiency also given by the compressor map (for more details on equation of motion refer to [4]).
The three section curves of the tested full-scale compressor have been tuned by matching dynamic simulation results with maximum and minimum direct/reverse flows measured during the surge tests. Fine tuning parameters used are the coordinates of minimum point of the dimensionless polytropic head $\Psi_{CC}$ at zero flow and coordinates of negative flow point at which the dimensionless polytropic head is equal to the one at surge limit (see Figure 12).

*5.2 Dynamic Simulation Model*

With reference to the actual gas loop (Figure 3), a compressor loop dynamic model has been built with a detailed characterization of all the testing equipment such as valves, piping, coolers, etc.
The software used was Aspen HYSYS® configured with the Peng-Robinson equation-of-state and Lee-Kesler option for the calculation of enthalpies. The standard Aspen HYSYS® compressor element has been replaced by a custom element able to correctly simulate the behavior of the compressor in the Second Quadrant according to the model described in the previous section.
The compressor speed model used is given by a torque balance equation (Equation (3)) applied to the train, in which the inertia of all the elements composing the train (electric motor driver, gear box, couplings and compressor) and the speed controller acting on electric motor torque have been considered. Such a model also allowed simulating the speed fluctuation due to the variations of both absorbed torque by the compressor and available torque from the electric motor.

$$\frac{\partial \omega}{\partial t} = \frac{\frac{T_{EM}}{GR} - T_{CC} - f \cdot \omega}{I_{TOT}} \qquad \textbf{Eq. 3}$$

In the dynamic model, the speed controller has been tuned to have its action on the Electric Motor Torque ($T_{EM}$) be able to reproduce the speed variation experienced during full speed tests. However, it should be noted that the main parameter affecting the speed variation in Equation (3) is the compressor absorbed torque ($T_{CC}$), which is calculated by the custom compressor element using the aforementioned curves.

The compressor loop dynamic model was first validated matching the initial steady state condition of each test run in terms of suction and discharge pressure, temperature, mass and volumetric flow of each compressor stage, and then used to replicate data obtained in the tests where surge events were induced on compressor sections 1, 2 and 3 (separately) at full speed and upon ESD with all recycle valves kept at their initial opening position. Data validation results are presented in the next section.

*5.3 Simulation data validation*

Data validation study results are shown in Figure 13, Figure 14, Figure 15 and Figure 16 for the four runs analyzed. Variables under investigation in this study are: mass flows, suction and discharge pressure in each compressor section and train speed. Compressor suction and discharge temperatures have not been included in this analysis as the relatively slow temperature probe response time and thermal inertia of the system do not adequately respond to the dynamics of a fast event like surge.
Although all the variables mutually influence each other, it is not possible to analyze them individually. Data validation of a single variable can give an indication of the accuracy of a particular part of the dynamic model.
A good alignment of pressure data in both full speed and emergency shut-down tests is mainly an indication that valves and all volumes of the gas loops have been simulated correctly.
Train speed predictability mainly indicates the capability to model the compressor speed control system and accuracy of the torque balance equation. Model accuracy in predicting train speed can be better assessed in the full speed tests, where the compressor speed control system is active and modulating electric motor delivered torque. In order to achieve a good speed matching, an accurate estimation of compressor absorbed torque is necessary, especially in the Second Quadrant. In the First Quadrant, the Torque can be calculated as follows:

$$T_{CC} = \frac{\frac{H_{pol,CC}}{\eta_{pol}} \cdot \dot{m}}{\omega} \qquad \textbf{Eq. 4}$$

In the Second Quadrant, Equation (4) can be considered to still be valid. As soon as the operating point shifts to the Second Quadrant, the absolute values of polytropic head and efficiency do not vary significantly, while the mass flow decreases to almost 10-20% of the steady state flow condition (see Figure 13, Figure 14, Figure 15 and Figure 16). Hence, in full speed tests, when the operating point moves to the Second Quadrant, the compressor absorbed torque decreases significantly leading, according to the torque balance equation (Equation (3)), to an increase in the compressor speed. This behavior has been correctly caught by dynamic simulation, as shown in Figure 13, Figure 14 and Figure 15 (black lines).
Finally, the predictability of mass flow processed by each compressor section is an indication of the accuracy of the model of the compressor itself.
As highlighted above, when the operating point is recovering from a reverse flow condition, i.e. flow processed by the compressor is increasing, the train also experienced a speed increase. Since speed has a direct influence on the compressor generated head (compressor generated head is proportional to the square of the speed), the equation of motion (Equation (2)) is also affected: the greater the compressor generated head, the higher the derivative of flow and so the less time is spent in the second quadrant.

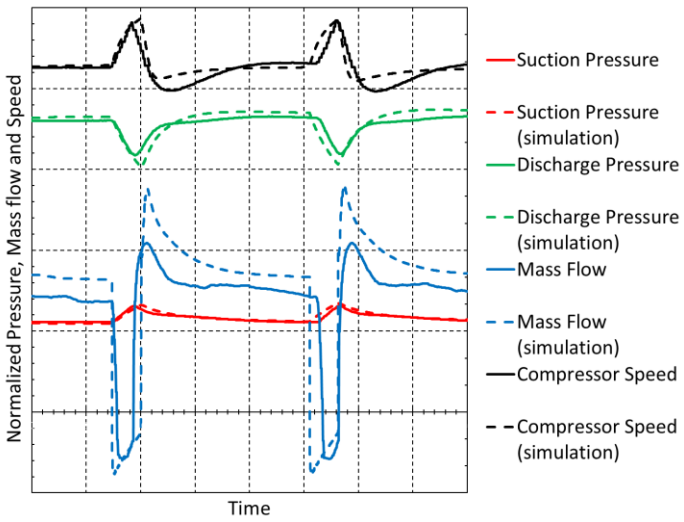


**Figure 13. Surge tests data validation between dynamic simulation and test data – Section 1 surge at full speed**

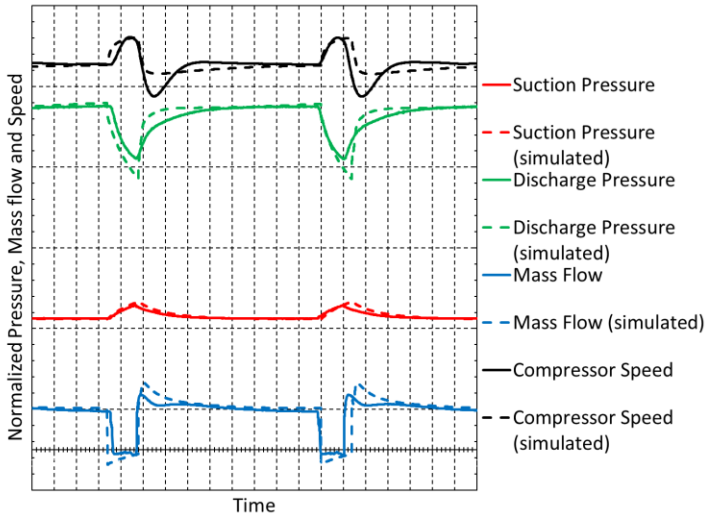


**Figure 14. Surge tests data validation between dynamic simulation and test data – Section 2 surge at full speed**

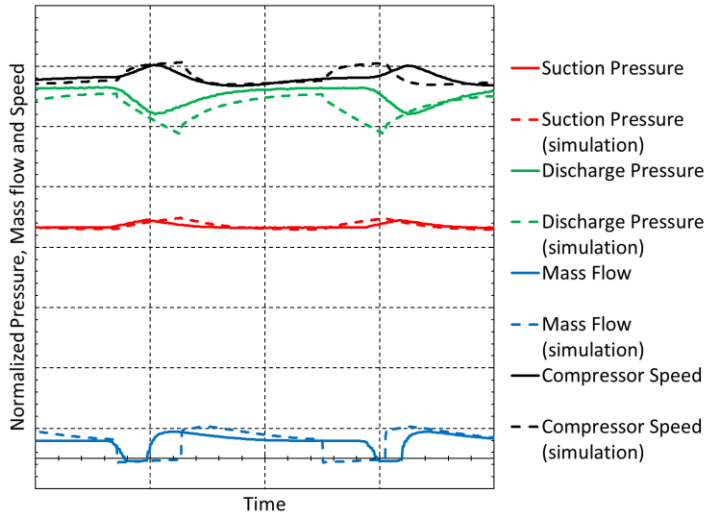


**Figure 15. Surge tests data validation between dynamic simulation and test data – Section 3 surge at full speed**

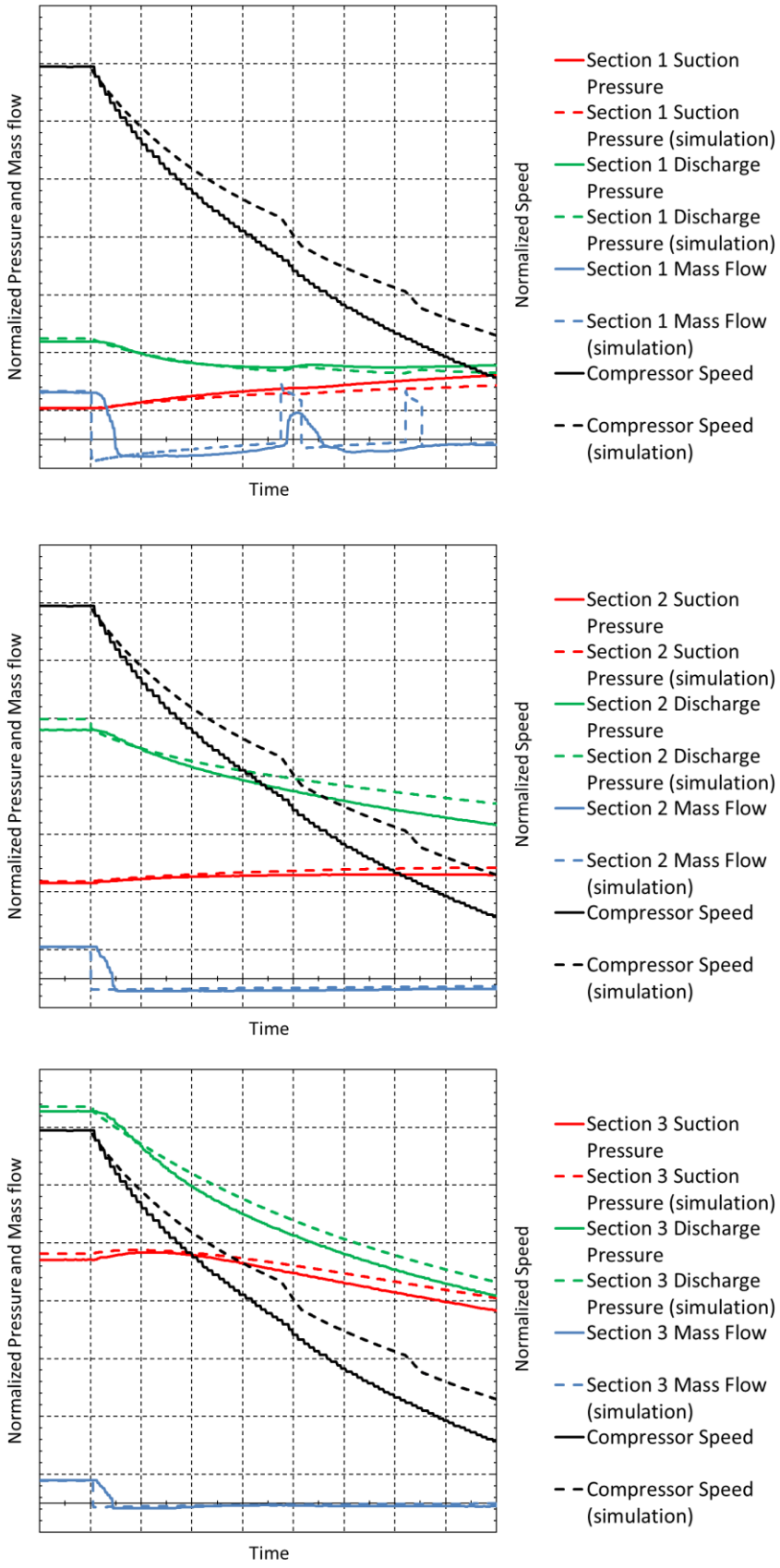


**Figure 16 Surge tests data validation between dynamic simulation and test data – ESD with Recycle Valves frozen**

Derivative of flow and the associated time spent in the second quadrant is also affected by the process polytropic head and so by the rate of suction/discharge pressures equalization which is strongly dependent on plant volumes, reverse mass flow through the compressor and mass flow passing through the recycle valves. This leads to the conclusion that all the variables of the compressor loop have an influence on surge cycle parameters: reverse flow duration, number of cycles and maximum and minimum direct/reverse flows. Since these are the key parameters on which the surge assessment of the machine during ESD is based, a good dynamic simulation model, capable of correctly predicting all the variables that describe the compressor loop behavior during both normal running and ESD scenarios, is essential to properly design surge protection devices.
Looking at tests results data validation from a surge cycle parameters standpoint, it can be observed that:

- maximum and minimum direct/reverse flows were the parameters fitted in the tuning process of the three compressor stage curves. Indeed, the simulated values almost perfectly fit the field data;
- time spent in reverse flow has been fairly matched in section 1 and 2 surge at full speed and ESD tests (within 20% difference), while it has been overestimated in section 3 surge at full speed test (+70%);
- number of surge cycle predictability can be assessed only in the ESD scenario. In this test, second and third compressor sections coast down occurred in reverse flow condition consistently with the test run; even the timeframe relevant to the first section excursion in the Second Quadrant is matched exactly as per Figure 16. The dynamic simulation tended to overestimate the number of surge cycles upon coast down (for section 1, simulation estimated 2 surge cycles instead of only 1), leading to a more conservative analysis of the ESD event.

## 6 CONCLUSIONS

Surge exploration tests on a full-scale centrifugal compressor have been performed allowing for an assessment of the machine design robustness and data collection in reverse flow operation. The tests have been carried out on different scenarios of gas loop pressurization and control action on recycle valves, in order to differentiate the surge severity.
An important outcome is that the reverse flow condition can be withstood by the compressor for any amount of time, since vibrations and axial thrust trends decayed smoothly during the compressor coastdown without any significant peaks in the amplitude and increased only when moving from Second Quadrant back into First Quadrant with a positive flow, as shown in Figure 4, 5, 7, and 8. However, surge phenomena associated with the change in rapidly oscillating gas flow, requires that a threshold on the number of surge cycles shall be taken into account to avoid undesirable consequences due to pressure waves and vibrations. Therefore, a new ESD surge acceptance criterion considering three surge cycles as threshold has been developed, instead of a maximum allowable operating time beyond the compressor SLL.
Data validation between surge exploration tests and dynamic simulations, along with the characterization of the Second Quadrant branch, allowed for the enhancement and fine tuning of the capability of transient compressor modelling. A good level of consistency between the main parameters affecting the transient compressor operability has been demonstrated. With the aid of this activity, a more accurate evaluation of compressor surge and reverse flow parameters (especially the number of surge cycles) is achieved whenever a dynamic simulation is performed on a particular compressor application.
Surge exploration test result analysis and dynamic modeling enhancement have been a breakthrough for the introduction of a new surge acceptance criterion based on number of surge cycles instead of time spent in the Second Quadrant, with expected benefits in reducing the complexity of surge protection devices (such as Hot Gas Bypass Valve or Cold Gas Bypass Valves) and associated costs, whilst still maintaining the safe operation of the compressor and related compressor system equipment.

## NOMENCLATURE

*Variables*

| | | |
|---|---|---|
| $\omega$ | = Compressor speed | ($t^{-1}$) |
| $t$ | = Time | (t) |
| $T$ | = Temperature, Torque | (T, $M \cdot L^2 \cdot t^{-2}$) |
| $GR$ | = Gear Ratio | (-) |
| $f$ | = Friction Loss factor of the train | ($M \cdot L^2 \cdot t^{-1}$) |
| $I_{TOT}$ | = Train total Inertia | ($M \cdot L^2$) |
| $\tau$ | = Work coefficient | (-) |
| $u$ | = Peripheral speed | ($L\ t^{-1}$) |
| $D$ | = Impeller diameter | (L) |
| $\varphi$ | = Flow coefficient | (-) |
| $\dot{m}$ | = Mass flow rate | ($M \cdot t^{-1}$) |
| M | = Mass | (M) |

| | | |
|---|---|---|
| L | = Length | (L) |
| $\rho$ | = Mass density | ($M \cdot L^{-3}$) |
| $r$ | = Pressure ratio | (-) |
| $P$ | = Total Pressure | ($M \cdot L^{-1} \cdot t^{-2}$) |
| H | = Head | ($L^2 \cdot t^{-2}$) |
| $\eta$ | = Efficiency | (-) |
| $\Psi$ | = Dimensionless polytropic head | (-) |
| $Mu$ | = Mach number | (-) |

*Subscripts*

| | |
|---|---|
| *EM* | = Electric Motor |
| *CC* | = Centrifugal Compressor |
| *P* | = Process |
| Des | = Design |
| *pol* | = Polytropic |
| *2* | = Section at the external diameter of the impeller |

*Acronyms*

| | |
|---|---|
| BHGE | = Baker Hudges a GE Company |
| HSS | = High Speed Shaft |
| DE | = Driver End |
| NDE | = Non-Driver End |
| ASV | = Anti Surge Valve |
| ESD | = Emergency Shut-Down |
| SLL | = Surge Limit Line |
| 1xRev | = Revolution Frequency |

**REFERENCES**


[1] API Standard 617, "Axial and Centrifugal Compressors and Expander-compressors", 8th edition, September 2014

[2] Belardini E., Tapinassi L., Rubino D.T., Pelella M., 2015, "Modeling of Pressure Dynamics During Surge and ESD", @ 3rd Middle East Turbomachinery Symposium

[3] Belardini E., Rubino D.T., Tapinassi L., Pelella M., 2016, "Four Quadrant Centrifugal Compressor Performance", @ Asia Turbomachinery & Pump Symposium

[4] Greitzer E.M., 1976, "Surge and Rotating Stall in Axial Flow Compressors. Part I: Theoretical Compression System Model", Journal of Engineering for Power

[5] Greitzer E.M., 1976, "Surge and Rotating Stall in Axial Flow Compressors. Part II: Experimental Results and Comparison with Theory", Journal of Engineering for Power

[6] Baldassarre L., Bernocchi A., Rizzo E., Fontana M., Maiuolo F., 2015, "Axial Thrust in High Pressure Centrifugal Compressors: Description of a Calculation Model Validated by Experimental Data from Full Load Test", @ 44th Turbomachinery & 31st Pump Symposia